The anatomical position of the ribs and thoracic vertebrae of the Roc de Marsal Neandertal infant

Asier Gómez-Olivencia[a,b,c,1,*], Daniel García-Martínez[d,e,1]

[a] Dept. Geología, Facultad de Ciencia y Tecnología, Universidad del País Vasco/Euskal Herriko Unibertsitatea (UPV/EHU). Barrio Sarriena s/n, 48940 Leioa, Spain
[b] Centro Mixto UCM-ISCIII de Evolución y Comportamiento Humanos. Avda. Monforte de Lemos, 5. Madrid 28029, Spain
[c] Sociedad de Ciencias Aranzadi, Zorroagagaina 11, 20014 Donostia-San Sebastián, Spain.
[d] Physical Anthropology Unit, Department of Biodiversity, Ecology, and Evolution, Faculty of Biological Sciences, Complutense University of Madrid, Madrid, Spain.
[e] Laboratory of Forensic Anthropology, Centre for Functional Ecology, Department of Life Sciences, University of Coimbra, Calçada Martim de Freitas, 3000-456, Coimbra, Portugal.

[1] These authors contributed equally.

SUPPLEMENTARY MATERIAL

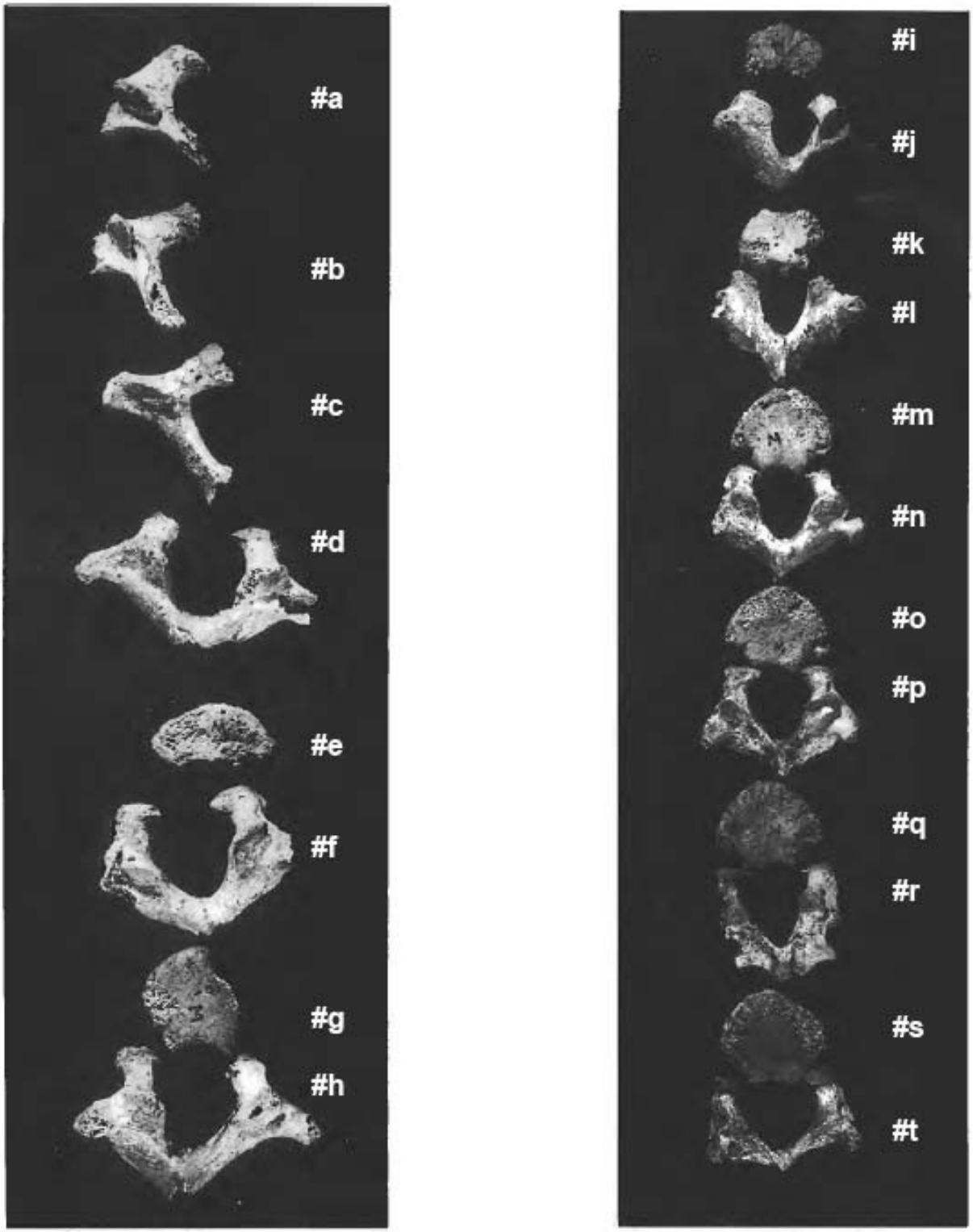

Figure S1

Virtual labelling of the Roc-de-Marsal 1 vertebrae following Madre-Dupouy's (1992) figure 28. The letters preceded by a "#" were added by us.

Figure S2

View of six rib shaft fragments associated with the Roc-de-Marsal 1 child skeleton for which it was impossible to make an anatomical determination.

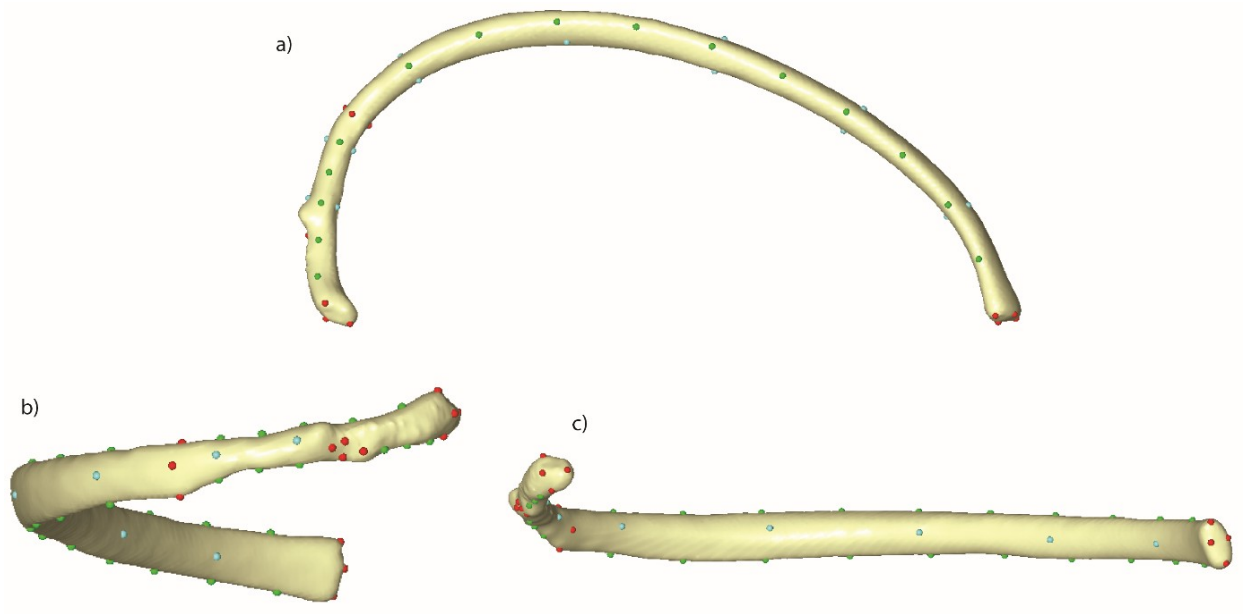

Figure S3

Quantification of the morphology of the 10th rib. Note that the rib on the figure is a 5th in cranial (a), posterior (b) and interior (c) views, but protocol remains the same. To quantify 10th rib morphology, four landmarks were measured at the cranial-, caudal-, medial- and lateral-most points of the rib head, and four landmarks were measured at the cranial-, caudal-, medial- and lateral-most points of the articular tubercle. Other four landmarks were placed at the posterior angle, two of them were located in the cranio-caudal dimension at the caudal- and cranial-most point at the maximum distance following the shaft maximum diameter at the angle (SMXD; Franciscus and Churchill, 2002) and the other two were located in the medio-lateral dimension at the medial- and lateral-most point at the maximum distance following the shaft minimum diameter at the angle (SMND; Franciscus and Churchill, 2002). Other four landmarks internal-, external-, superior- and inferior-most points of the sternal end. To better quantify rib curvature and shaft height we used the following semilandmark approach: Lower costal border - three equidistant curve semi-landmarks were located between the inferior-most point of the rib head and the medial-most point of the articular tubercle; three equidistant curve semi-landmarks were located between the lateral-most point of the articular tubercle and the caudal-most point of the posterior angle cross-section; 10 equidistant curve semi-landmarks were located between caudal-most point of the posterior angle cross-section and the caudal-most point of the distal end. Upper costal border – five equidistant curve semi-landmarks were located between the superior-most point of the rib head and the cranial-most point of the posterior angle cross-section. 10 equidistant curve semi-landmarks were located between the cranial-most point of the posterior angle cross-section and the cranial-most point of the distal end. External surface – two surface semi-landmarks were equidistantly located at the external surface of the rib shaft following the midline of it from the lateral-most point of the rib head to the lateral-most point of the posterior angle cross-section; five surface semi-landmarks were equidistantly located at the external surface of the rib shaft following the midline of it from the lateral-most point of the posterior angle cross-section to the lateral-most point of the distal end. Internal surface – two surface semi-landmarks were equidistantly located at the internal surface of the rib shaft following the midline of it from the medial-most point of the rib head to the medial-most point of the posterior angle cross-section; five surface semi-landmarks were equidistantly located at the internal surface of the rib shaft following the midline of it from the medial-most point of the posterior angle cross-section to the medial-most point of the distal end. Each 5th rib was thus described by 61 3D landmarks.

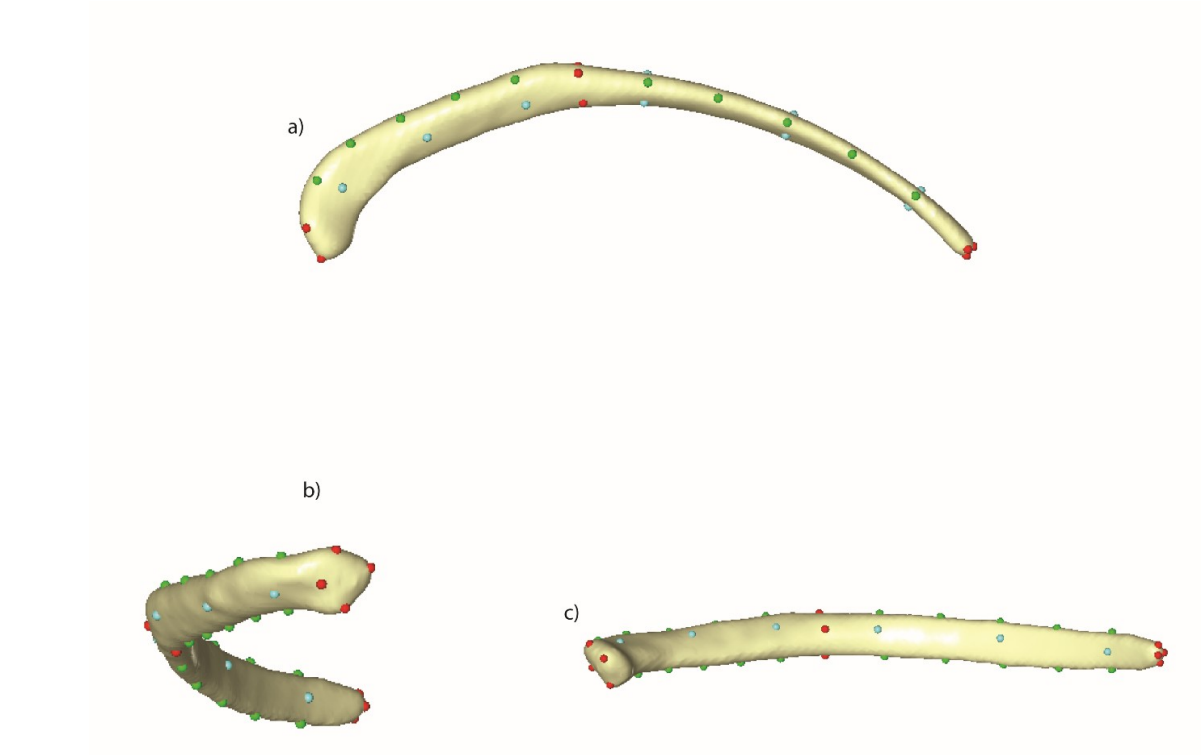

Figure S4

Quantification of the morphology of the 11th rib in cranial (a), posterior (b) and interior (c) views. Four landmarks were measured at the cranial-, caudal-, medial- and lateral-most points of the rib head. Four landmarks were placed at the posterior angle, two of them were located in the cranio-caudal dimension at the caudal- and cranial-most point at the maximum distance following the shaft maximum diameter at the angle (SMXD; Franciscus and Churchill, 2002) and the other two were located in the medio-lateral dimension at the medial- and lateral-most point at the maximum distance following the shaft minimum diameter at the angle (Franciscus and Churchill, 2002). Other four landmarks internal-, external-, superior- and inferior-most points of the sternal end. To better quantify rib curvature and shaft height we used the following semilandmark approach: Lower costal border - five equidistant curve semi-landmarks were located between the inferior-most point of the rib head and the caudal-most point of the posterior angle cross-section; five equidistant curve semi-landmarks were located between caudal-most point of the posterior angle cross-section and the caudal-most point of the distal end. Upper costal border – five equidistant curve semi-landmarks were located between the superior-most point of the rib head and the cranial-most point of the posterior angle cross-section. Five equidistant curve semi-landmarks were located between the cranial-most point of the posterior angle cross-section and the cranial-most point of the distal end. External surface – Three surface semi-landmarks were equidistantly located at the external surface of the rib shaft following the midline of it from the lateral-most point of the rib head to the lateral-most point of the posterior angle cross-section; three surface semi-landmarks were equidistantly located at the external surface of the rib shaft following the midline of it from the lateral-most point of the posterior angle cross-section to the lateral-most point of the distal end. Internal surface – three surface semi-landmarks were equidistantly located at the internal surface of the rib shaft following the midline of it from the medial-most point of the rib head to the medial-most point of the posterior angle cross-section; three surface semi-landmarks were equidistantly located at the internal surface of the rib shaft following the midline of it from the medial-most point of the posterior angle cross-section to the medial-most point of the distal end. Each 11th rib was thus described by 44 3D landmarks.

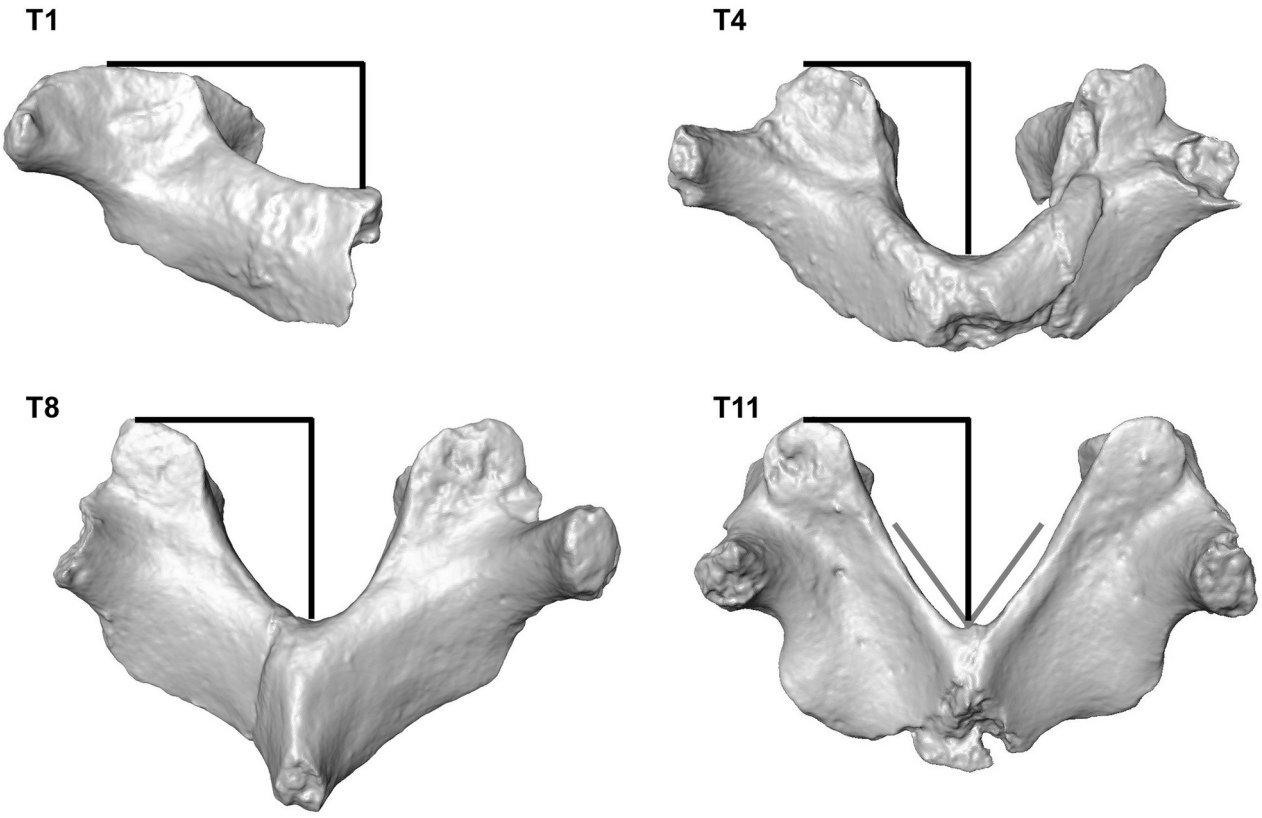

Figure S5

Dorsal view of selected thoracic vertebrae from Roc de Marsal. Note the increase in vertical distance between the cranial edge of the upper articular facets and the cranial end of the union of the laminae from cranial to caudal. Additionally the relative position between the articular facet and the transverse process also changes, especially from T1 (at approximately the same height) to T4 (the articular facet is more cranial than the transverse process) and the union of the laminae becomes more 'V' shaped in the caudal-most thoracic vertebrae.

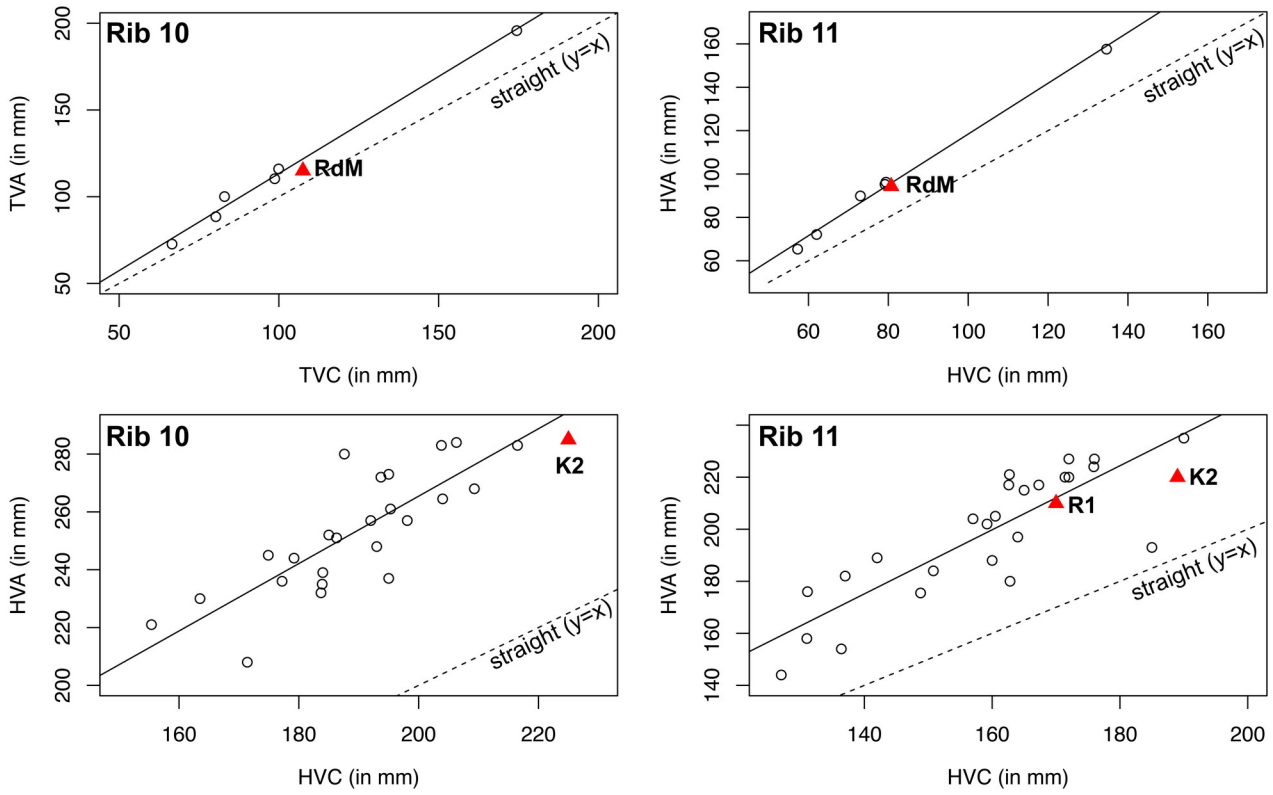

Figure S6

General curvature of the 10th and 11th ribs in Neandertals compared to modern humans. Top row: Roc de Marsal (RdM) infant compared to *Homo sapiens* infants. Bottom row: Kebara 2 (K2) and Regourdou 1 (R1) compared to *Homo sapiens* adults. HVA = head-ventral arc; HVC = head-ventral chord; TVA = tubercle-ventral arc; TVC = tubercle-ventral chord (Gómez-Olivencia et al., 2010). The infant measurements are derived from (semi)landmarks.

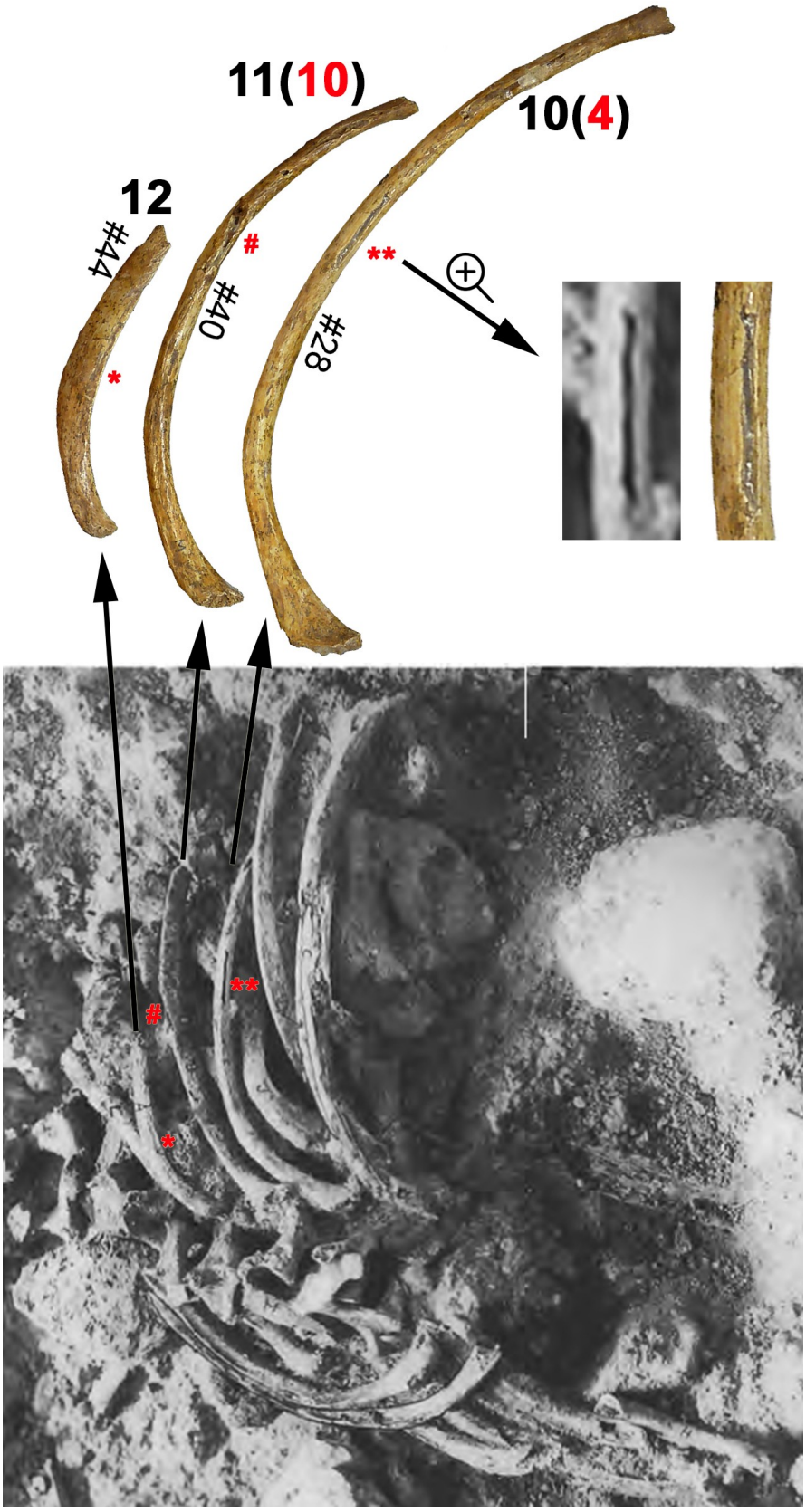

Figure S7

Comparison of the last three ribs from the left side (following our seriation) to an image of the thorax of Roc de Marsal when it was being cleaned, with the ribs in anatomical position (Madre-Dupouy, 1992). Note that it is possible to observe certain anatomical and taphonomic features (*, #, **) that support the re-assessment of the anatomical position of the 10th and 11th ribs.

Figure S8

Comparison (caudal view) of Neandertal adult ribs 9–11 from Kebara 2 (K2) and Regourdou 1 (R1) to the male individual HTH 1674 from the Hamann-Todd collection. Note that, when lying on a table, the external surface of the Neandertal ribs is more vertical while in modern humans it is oriented more medially. This is likely related to the general geometry of the thorax in which the ribs of Neandertals are more horizontally oriented while modern humans show less declined ribs. Also note the larger articular tubercle of the 9R of Kebara 2 (Gómez-Olivencia et al., 2019).

Table S1

Raw dimensions (in mm) of the neural arch of the thoracic vertebrae of the Roc de Marsal Neandertal infant.[a]

Virtual label[b]	Serial position		Vertebral foramen width (M11)	Pedicle		Bi-articular diameter (r/l)	Transverse Diameter		Lamina	
	This study	Madre-Dupouy, 1992		height (r/l)	thickness (r/l)		Superior (Sup Tr Di)	Inferior (Inf Tr Di)	height (r/l)	thickness (r/l)
#c	T1	T3	-	-/4.1	-/4.4	-/12.6	-	-	-/8.0	-/4.0
#b	T2	T2	-	-/5.3	-/5.4	-/15.7	-	-	-/-	-/3.9
#a	T3	T1	-	-/5.6	-/4.9	-/16.9	-	-	-/-	-/-
#d	T4	T4	>11.9	6.0/5.9	4.9/4.8	17.8/-	(25.0)	(25.0)	-/-	-/3.6
#j	T5	T7	(12.5)	5.6/5.7	4.3/4.9	-/17.3	(22.5)	24.4	-/8.4	-/3.2
#l	T6	T8	-	-/-	-/-	-/17.7	(23.0)	25.8	8.6/-	3.6/-
#h	T7	T6	11.9	5.5/5.7	5.0/4.5	-/18.2	(23.8)	23.4	8.3/9.1	3.4/3.4
#n	T8	T9	13.2	6.3/6.3	4.8/5.2	18.2/18.2	24.2	25.4	9.2/8.8	3.6/3.4
#f	T9	T5	-	5.8/6.8	4.8/4.8	(19.5)/-	-	-	-/9.4	3.6/3.3
#o	T10	T10	-	7.5/7.4	5.2/5.8	20.2/19.4	-	-	9.1/-	3.3/3.2
#t	T11	T12	-	7.8/8.3	5.5/5.6	19.5/19.8	-	-	8.5/-	2.3/2.3
#r	T12	T11	-	8.1/7.9	6.0/4.9	22.6/23.3	-	-	-/11.6	-/1.9

[a] Values between parentheses are estimated.

[b] Underlined and bold labels indicate specimens in which our reinterpreted serial position differs from that published by Madre-Dupouy (1992).

Table S2

Anatomical determination and raw dimensions (in mm) of the ribs from the upper thorax of the Roc de Marsal Neandertal infant skeleton[a-b].

Variable	#26	#43.5	#33.2	#43.1	#41	#37(302)	#42	#31	#33.1	#38(302)	#30	#43.2	#39(302)	#34
	2L	2?L (11R)	3R (5R)	4?R	4?R (8R)	4R (8R)	4?R (11L?)	4L (3L)	5?R	5R (9R)	5L	6R (9R)	6R	6L
Preserved length	47.8	47.9	44.0	21.8	38.0	53.3	19.5	56.3	31.8	52.2	113.5	30.5	52.8	119.1
Preserved external arc	61.0	25.0	51.0	12.0	33.0	47.0	19.0	56.0	34.0	49.0	118.0	26.0	44.0	137.0
Preserved external arc ventral to the tubercle	41.0	25.0	51.0		33.0	47.0	19.0	56.0	22.0	49.0	118.0	17.0	44.0	137.0
Preserved internal arc	50.0	34.0	32.0	22.0	37.0	54.0	16.0	55.0	28.0	52.0	72.0	32.0	49.0	125.0
Head cranio-caudal diameter (HCCD)	4.9			(6.0)										
Shaft maximum cranio-caudal diameter at dorsal end (DSMxD)			4.6						5.0			5.5		6.2
Shaft minimum diameter (perpendicular to maximum cranio-caudal diameter) at dorsal end (DSMnD)			6.6						5.3			5.7		5.1
Shaft maximum cranio-caudal diameter at posterior angle (SMxD)			4.7						6.4					7.4
Shaft minimum (perpendicular to maximum cranio-caudal diameter) diameter at posterior angle (SMnD)			7.0						4.8					5.2
Mid-shaft maximum[c] diameter (MMxD)	3.7				7.5	7.8							6.7	8.1
Mid-shaft minimum[d] diameter (MMnD)	7.0				4.8	4.8							5.3	5.0
Sternal end maximum diameter (SEMxD)		(7.5)					[10.0]	9.6			[7.6]			
Sternal end minimum diameter (SEMnD)		(5.0)					[4.6]	5.2						

Numbering of the variables follows Gómez-Olivencia et al. (2010).

[a] In those instances in which our anatomical determination differs from that published by Madre-Dupouy (1992), it has been placed in parentheses. The measurements of the shaft fragments from #302 were taken at the mid-shaft of the preserved portion.

[b] Values in parentheses are estimated. Values between [] are the preserved values and thus must be considered a minimum.

[c] Measured in cranio-caudal direction.

[d] Measured in internal-external direction.

Table S3

Anatomical determination[a] and raw dimensions (in mm) of the ribs from the lower thorax of the Roc de Marsal Neandertal child skeleton[a-b].

Variable	#35	#36	#32	#43.3	#28	#27	#40	#43.4	#44
	7R	8L (7L)	9R (6R)	10R	10L (4L)	11R (4R)	11L (10L)	12R	12L
Preserved length	122.3	112.9	118.0	72.2		69.1		53.6	48.5
Preserved external arc	143.0	148.0	140.0	65.0		71.0		56	53.0
Preserved external arc ventral to the tubercle	143.0	136.0	136.0	58.0	122.0	71.0		56	53.0
Preserved internal arc	136.0	129.0	135.0	79.0	126.0	66	94.0	53.5	46.0
Tuberculo-ventral chord (TVC)									
Head-ventral chord (HVC)					110.0		83.3		
Tuberculo-ventral arc (TVA)									
Head-ventral arc (HVA)					132.0		98.0		
Head cranio-caudal diameter (HCCD)		(6.5)							5.3
Total neck length (TNL)		15.6							
Neck minimum cranio-caudal diameter (NMnCCD)		5.2							
Neck thickness (NTh)		6.7							
Articular tubercle height (ATH)		4.5	4.7						
Articular tubercle width (ATW)		7.2							
Tubercle-iliocostal line distance 2 (TID2)		(30.0)	(33.0)						
Shaft maximum cranio-caudal diameter at dorsal end (DSMxD)	6.0	6.7	6.0	5.3	5.3		4.0	3.6	3.7
Shaft minimum diameter (perpendicular to maximum cranio-caudal diameter) at dorsal end (DSMnD)	4.8	5.2	4.5	5.0	4.1		4.4	4.3	4.2
Shaft maximum cranio-caudal diameter at posterior angle (SMxD)			(7.8)	7.5	7.7		6.7	6.1	6.6
Shaft minimum diameter (perpendicular to maximum cranio-caudal diameter) at posterior angle (SMnD)	4.7	4.8	4.3	3.9	4.1		3.9	3.3	3.1
Mid-shaft maximum diameter (MMxD)	8.5	9.3	8.7		7.4	6.9	6.1		
Mid-shaft minimum diameter (MMnD)	4.3	4.0	3.6		3.6	3.5	3.4		
Sternal end maximum diameter (SEMxD)			(8.0) [7.8]		(7.1)		(6.1)		
Sternal end minimum diameter (SEMnD)			[4.5]		(5.1)		3.3		

Numbering of the variables follows Gómez-Olivencia et al. (2010).

[a] In those instances in which our anatomical determination differs from that published by Madre-Dupouy (1992) it has placed in parentheses.

[b] Values in parentheses are estimated. Values between [] are preserved values.

References

Franciscus RG, Churchill SE (2002) The costal skeleton of Shanidar 3 and a reappraisal of Neandertal thoracic morphology. J Hum Evol 42:303–356. https://doi.org/10.1006/jhev.2001.0528

Gómez-Olivencia A, Carretero JM, Lorenzo C, et al (2010) The costal skeleton of *Homo antecessor*: preliminary results. J Hum Evol 59*:*620–640. https://doi.org/10.1016/j.jhevol.20

Gómez-Olivencia A, Holliday T, Madelaine S, et al (2019) The costal skeleton of the Regourdou 1 Neandertal. J Hum Evol 130*:*151–171. https://doi.org/10.1016/j.jhevol.2017.12.005

Madre-Dupouy M (1992) L'enfant du Roc de Marsal. Éditions du CNRS, Paris.